

Towards a Novel Generation of Haptic and Robotic Interfaces: Integrating Affective Physiology in Human-Robot Interaction

M. Bianchi^{1,2,*}, G. Valenza¹, A. Greco¹, M. Nardelli¹, E. Battaglia¹, A. Bicchi^{1,2}, and E.P. Scilingo¹ .

Abstract—Haptic interfaces are special robots that interact with people to convey touch-related information. In addition to such a discriminative aspect, touch is also a highly emotion-related sense. However, while a lot of effort has been spent to investigate the perceptual mechanisms of discriminative touch and to suitably replicate them through haptic systems in human robot interaction (HRI), there is still a lot of work to do in order to take into account also the emotional aspects of tactual experience (i.e., the so-called *affective haptics*), for a more naturalistic human-robot communication. In this paper, we report evidences on how a haptic device designed to convey caress-like stimuli can influence physiological measures related to the autonomous nervous system (ANS), which is intimately connected to evoked emotions in humans. Specifically, a discriminant role of electrodermal response and heart rate variability can be associated to two different caressing velocities, which can also be linked to two different levels of pleasantness. Finally, we discuss how the results from this study could be profitably employed and generalized to pave the path towards a novel generation of robotic devices for HRI.

I. INTRODUCTION

Touch represents one of the primary sensory modalities in humans, which drives cognitive developments from the early phases of our infancy [1]. In addition to such a discriminative role, which has been widely studied in the literature [2], touch was also proven to provide affective inputs to human brain [3], which are crucial for emotion-related communication and social interactions [4]. Under this regard, touch not only can communicate the hedonic tone of emotions but also acts as an emotion-intensifier. Considering pleasantness perception, different haptic properties seem to play a crucial role, e.g. surface roughness, softness and smoothness, among the others [5], and they can be related to user's gender, age as well to body site of stimulation [6], [7]. These findings have hence driven the development of artificial systems that are able to convey haptic stimuli capable to influence the emotional state of users [8]–[10].

In [11], we presented an affective device able to administer caress-like (thus emotional) stimuli. The system allows controlling both the velocity of the caress-like movement and the strength of the caress. We then performed a preliminary psycho-physiological test involving 6 participants to determine the device capability of eliciting tactually emotional states in humans. To categorize emotions, we used the Circumplex Model of Affect (CMA) [12], [13], which allows taking into account two main dimensions conceptualized by the terms of valence and arousal, the first related to

pleasure/displeasure and the other to alertness. Moreover, we evaluated the activation of the Autonomic Nervous System (ANS), which is intimately connected to evoked emotions in humans [14], through the analysis of the electrodermal response (EDR). We found a statistically significant correlation between the perceived arousal level and the strength of the caress and between the perceived valence level and the velocity of the caress. Moreover, we found that phasic EDR was able to discern between pleasant and unpleasant stimuli. The main conclusions that can be drawn from these preliminary results are that it is possible to use physiological ANS-related quantities to distinguish between pleasant and unpleasant haptic stimulation.

In this paper, we push forward the investigation of ANS elicitation through caress-like haptic stimuli in [11]. More specifically, to get an exhaustive characterization of ANS response, we performed a completely new set of acquisitions and analyses with a large number of participants (32, 16 females), taking into account both EDR and cardiovascular dynamics, the latter one estimated through Heart Rate Variability (HRV) series. These series are representative of sympathetic and parasympathetic functions of ANS, respectively. More specifically, HRV refers to the variability of the time interval between two heartbeats, identified by R-waves from the Electro-CardioGraphy (ECG) signals, and has been extensively used in studies related to affective computing [15]. For example, after massage, changes in the parasympathetic activity estimated through spectral HRV analysis were observed [16]. We will here provide a comprehensive assessment of ANS, considering HRV linear and nonlinear dynamics during caress-like stimuli on the forearm, along with EDR measures obtained after applying a deconvolutive method to separate tonic and phasic components [17]. We will show how such ANS related quantities can be associated to different emotional states described through CMA and used to discriminate different physical quantities for the conveyed stimuli. More specifically, we will focus on different values of the velocity of the simulated caress at a given level of the conveyed force. We will also discuss how these results could be profitably applied for the design of a novel category of haptic interfaces and robotic systems, with special focus on rehabilitation robotics and assistive devices. These new interfaces will be able to integrate affective physiology within the control loop, thus modifying the control inputs according to the emotional state of the user.

II. SYSTEM DESCRIPTION

The affective haptic display [11] used in this study exploits the elasticity of a fabric to reproduce haptic stimuli that are commonly conveyed through the human caress. More

¹ Research Centre “E. Piaggio”, University of Pisa, Largo L. Lazzarino, 1, 56126 Pisa, Italy

² Department of Advanced Robotics, Istituto Italiano di Tecnologia, via Morego, 30, 16163 Genova, Italy.

* Corresponding Author: matteo.bianchi@centropiaggio.unipi.it

specifically, the user places the forearm on a support under the fabric layer, whose extremities are connected to two rollers that can be moved by two motors. By controlling motor positions and rotation velocity, it is possible to vary the velocity and the strength of the artificial caress on the user arm. The system is also endowed with a load cell that measures the normal force exerted by the fabric on the forearm. After a calibration phase, where the offset due to the forearm weight is removed, the exerted force (i.e. the strength of the caress) can be varied by acting on the two motor positions, which determine how much the fabric is wrapped around the forearm and hence the force exerted on it (maximum force 20 N). Once the desired level of force is achieved, and both motors are in the reference position, the velocity of the caress can be modulated by regulating the velocity of the motors, exploiting a built-in motor position controller and feeding the motors with a sinusoidal input reference trajectory. By setting the frequency and amplitude of the input, we can control the velocity and the amplitude of motor rotation, respectively. The maximum angular displacement of the motors from the reference positions is set to $\pm 90^\circ$, while an entire control cycle lasts 1 ms. An overview of the system is shown in Fig. 1, including the envisaged embedded front-end to directly acquire and process physiological signals. For further technical details on the device, the reader is invited to refer to [11].

It is important to note that the leading idea for the design of the system is to convey distributed tactile stimuli related to velocity and pressure cues, which are commonly delivered through human caress, and to assess whether such stimuli could elicit an affective response in users. Similarity between artificial stimulation and human-mediated one will be investigated in future works.

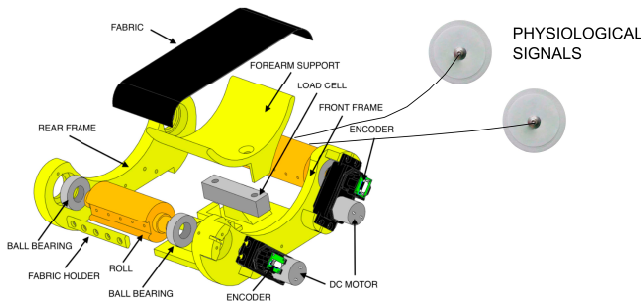


Fig. 1: The main components of the affective haptic device and the envisaged front end for the acquisition of the physiological signals from the user.

III. MATERIALS AND METHODS

The goal of this study was twofold: (i) to assess a discriminant role of HRV and EDR associated with two simulated caressing velocities; (ii) to link such a role to given evoked emotions categorized through stimulus self-assessment. We chose to focus on the velocity parameter since the inverse relationship between the velocity value and pleasantness level was already demonstrated in literature [6], [11]. To pursue objective (i), we extracted features from the signal time series of HRV and EDR, to investigate their sensitivity to changes in caressing velocity.

A. Subject Recruitment and Experimental protocol

Thirty-two healthy subjects naive w.r.t experimental goals aged 27 ± 2 (16 males, age 26 ± 2 , and 16 females, age 27 ± 2) gave their informed consent to take part in the study. The study was previously approved by the local Ethical Committee. Subjects were informed that during the experimental procedure they would have experienced a set of haptic stimuli and that, at the end of each stimulus, they would have gone with the self-assessment procedure described in the following section. Throughout the experiment, participants wore earplugs in order to prevent any auditory cue and were asked to keep their eyes closed. Only during the self assessment phase, they were allowed to open their eyes, but a panel still prevented them from seeing the device that was delivering caress-like stimuli. Prior to the experiment, the device load cell was calibrated with respect to the forearm weight for each participant.

Keeping the level of force constant to 6 N, we used two different caressing stimuli related to 2 levels of velocity ($V_1=9.4$ mm/s, $V_2=37$ mm/s). Each stimulus consisted of a back and forth caress-like movement of the fabric over the participant's forearm, which was obtained by giving a reference position to the motors (to achieve the desired level of force) and then feeding them with two different sinusoidal input trajectories, at the frequencies of 0.1 Hz and 0.4 Hz, respectively (for further details see [11]). These values were chosen according to previous studies [11], [18]. Between two consecutive stimuli, the motors were stopped and the force was set to 0 N. In this case, the fabric was only lightly in contact with the forearm. As the force increases, the fabric gets wrapped around the forearm and there is no more pure sliding (as with light forces) but also skin torsion. This behavior was coherent with the goal of reproducing as exhaustively as possible the behavior of the human caress. Throughout the experiment, there were two phases of resting sessions with a duration of two minutes: the first at the beginning of the protocol, the second at the end of the stimulation. Stimuli were randomized in time among subjects, with an inter-stimulus interval of 35 seconds.

B. Stimulus Self-Assessment and Acquisition set-up

For the stimulus self-assessment procedure, we also asked participants to report their emotional response to the stimuli conveyed by the device. For this reason, we adopted the Circumplex Model of Affect (CMA) [12], a common model to categorize emotions using two main dimensions conceptualized by the terms of valence and arousal. According to [12], in fact, affective states arise from two fundamental neurophysiological systems: one related to valence (pleasure/displeasure) and the other to arousal, or alertness. The connection between these two dimensions and ANS response was previously demonstrated [19].

Specifically, after each stimulus, participants were invited to indicate the level of arousal and valence through the Self Assessment Manikin (SAM) [20]. SAM is a pictorial assessment technique that directly measures the pleasure (valence) and arousal associated with a person affective reaction to stimuli. The SAM used for our experiments contains 10 items, 5 levels of arousal (i.e. from 1 to 5, in an

increasing scale, ranging from neutral to emotionally strong) and 5 levels for the valence (i.e. from -2 to 2, in a scale from highly unpleasant stimuli to highly pleasant stimuli, neutral level 0). During the elicitation, ECG and EDR signals were acquired using the BIOPAC acquisition system, with a sampling rate of 500 Hz.

C. HRV Signal Processing and Feature Extraction

According to the HRV processing guidelines [15], we chose to extract both standard and nonlinear features in order to characterize the autonomic control of the cardiovascular dynamics. Standard HRV analysis refers to the extraction of parameters defined in the time and frequency domain [21]. More specifically, time domain features include statistical parameters and morphological indexes. We calculated the following indexes:

- the first (*meanRR*) and second order moment (*SDNN*) of the RR intervals, i.e. the intervals between two consecutive R waves (so-called normal-to-normal, *NN*, intervals);
- the square root of the mean of the sum of the squares of differences between subsequent *NN* intervals ($RMSSD = \sqrt{\frac{1}{N-1} \sum_{j=1}^{N-1} (NN_{j+1} - NN_j)^2}$, where *N* is the total number of heartbeats under investigation);
- the number of consecutive intervals that differ by more than 50 ms, *NN50*, expressed as a percentage of the total number of heartbeats *N* analyzed ($pNN50 = \frac{NN50}{N-1} 100\%$)

We also estimated the triangular index (*TINN*), which is defined as the base of the triangle that best approximates the *NN* interval distribution (the minimum square difference is used to find such a triangle).

We also calculated several features in the frequency domain from the Power Spectral Density (PSD) analysis. PSD was estimated with the Welch's periodogram, which relies on the FFT (Fast Fourier Transform) algorithm. Three spectral bands can be defined as follows: *VLF* (very low frequency) with spectral components below 0.04 Hz; *LF* (low frequency), ranging from 0.04 to 0.15 Hz; *HF* (high frequency), comprising frequencies between 0.15 to 0.4 Hz. For each of these three frequency bands, we also evaluated: the frequency having maximum magnitude (*VLF_{peak}*, *LF_{peak}*, and *HF_{peak}*, respectively); the power – expressed as percentage of the total power – (*VLF_{power%}*, *LF_{power%}*, and *HF_{power%}*, respectively); the power normalized to the sum of the LF and HF power. Moreover, we calculated the LF/HF power ratio.

Furthermore, we also considered nonlinear indices extracted from HRV series, relying on two methods: *Symbolic Analysis* and the *Lagged Poincaré Plot (LPP)* [15], [22], [23].

- *Symbolic analysis*: it is based on the conversion of the series into a sequence of symbols [23], [24]. According to the specific literature [23], [24], each HRV series was divided in six levels of amplitude and a numeric symbol (from 0 to 5) was assigned to each data sample according to the amplitude level of belonging. In this way, data were converted in symbolic series and we investigated on the trend of patterns constituted by three consecutive symbols. The patterns of three symbols were divided into five classes: 0V, patterns with no

variations, where all symbols were equal; 1Va, patterns with one variation in the amplitude level of belonging, where the variation was between the second and the third symbol; 1Vb, patterns with one variation, where the variation was between the first and second symbol; 2Va, patterns with two variations and with a trend strictly increasing or strictly decreasing; 2Vb, all the other patterns with two variations. We used as features the count of patterns in each class and their percentage values (%);

- *Lagged Poincaré Plot (LPP)*: this method quantifies the fluctuations of the dynamics of the time series through the scatter plot of *NN* intervals, where each *NN_n* interval is mapped as a function of the successive *NN_{n+M}*. In this study, we chose $1 \leq M \leq 10$ [22], [25], [26]. The features that can be extracted with the Poincaré Plot are:
 - *SD1*: the standard deviation related to the points that are perpendicular to the line-of-identity $NN_{n+M} = NN_n$. It describes the HRV short-term variability.
 - *SD2*: the standard deviation that describes the long-term dynamics and measures the dispersion of the points along the identity line.
 - *S* ($S = \pi \cdot SD1 \cdot SD2$): the area of an imaginary ellipse with axes *SD1* and *SD2*.

For each of the previous features, we built the graph in function of *M* and calculated the area under the curve (*AUC*) of the LPP:

- *AUC* value for lower values of *M* (*AUC_{low}*, $1 \leq M \leq 5$);
- *AUC* value for higher values of *M* (*AUC_{high}*, $5 \leq M \leq 10$);
- the ratio between *AUC_{low}* and *AUC_{high}* (*AUC_{low/high}*);
- the ratio between *AUC_{low}* and the total *AUC* for $1 \leq M \leq 10$ (*AUC_{low/tot}*);
- the ratio between *AUC_{high}* and the total *AUC* for $1 \leq M \leq 10$ (*AUC_{high/tot}*).

D. EDR Signal Processing and Feature Extraction

Electrodermal response (EDR) is the general term used to define autonomic changes in the electrical properties of the skin. One of the most frequently used measures of EDR is skin conductance (*SC*), which can be quantified by applying an electrical constant potential between two points of skin contact (usually the medial or distal phalanges of the non-dominant hand) and measuring the resulting current between them. The EDR signal can be divided into a slowly-varying component, the so-called tonic component (i.e. skin conductance level (*SCL*)), and a superposed phasic component, which is characterized by a shorter rise time and a slower recovery time (i.e. skin conductance response, *SCR*) [17], [27], [28]. Literature evidences suggest that these two components rely on different neural mechanisms [29] and, consequently, that both convey relevant and non-redundant information about the ANS activity. Indeed, *SCL* component contains information about the general physiological status of the subject and reflects general and slow changes in the

ANS dynamics [30]. The phasic component, *SCR*, instead, is linked to exogenous stimuli such as lights, sounds, smells, and is defined as a variation in the SC signal arising within a predefined response window (1 - 5 s after stimulus onset), exceeding a minimum amplitude criterion ($0.05\mu S$) [31]. Of note, phasic change features are reliable markers for the assessment of the flight-or-flight responses and are able to quantify the affective response of the subject during multi-sensory stimulations [32], [33]. Sometimes, there are some innate responses in the SC-curve, even without external stimuli. Those nonspecific skin conductance responses (*NsSCR*) have the same characteristics as stimulus-related SCRs, but are considered tonic measures because they occur in the absence of external stimuli. [34].

In this work, we processed the SC data by means of the Continuous Deconvolution Analysis (CDA) [35]. The EDR is modeled as a convolution of the ANS (i.e., sudomotor nerve activity (*SMNA*)) and an impulse response function called Bateman function, $h(t)$, described in eq. 2

$$EDR(t) = SMNA(t) \otimes h(t) \quad (1)$$

where:

$$h(t) = (e^{-\frac{t}{\tau_1}} - e^{-\frac{t}{\tau_2}}) u(t) \quad (2)$$

with $\tau_1 = 0.7$ s and $\tau_2 = 3$ s ($u(t)$ is the unitary step function and \otimes is the convolutive operator). In the eq. 3, *SMNA* is unknown and it is evaluated by deconvolving the EDR signal with the impulse response function ($h(t)$), after a preprocessing phase consisting of the visual detection and removal of the movement artifacts, and a low pass zero-phase filtering with a cutoff frequency of 2 Hz. The deconvoluted driver signal *SMNA* is the sum of the two components, tonic and phasic

$$SMNA = (DRIVER_{tonic} + DRIVER_{phasic}) \quad (3)$$

The hypothesis underling SC component behavior is that tonic activity is observable in the absence of any phasic activity [17]. Therefore, the $DRIVER_{tonic}$ component can be obtained through the application of a smoothing Gaussian window of 200 ms and a peak detection algorithm in order to find the peaks under a fixed threshold. The $DRIVER_{phasic}$ component, instead, can be computed by subtracting the previously estimated $DRIVER_{tonic}$ from the *SMNA*. More details can be found in [35]. Once the tonic and phasic components are estimated from the CDA model, several features can be extracted to investigate the sensitivity to changes in caressing velocity. According to specific literature [17], [35], we chose to extract the features described in Table I.

The following analyses were performed:

- *Event-related phasic analysis*: we studied EDR within a time response window of 5 s [17], [35] after the affective stimulus;
- *Tonic analysis*: we considered the mean tonic value during the caress-like stimulation and the mean tonic value differences between the post- and pre-stimulus sessions.

TABLE I: List of features extracted from EDR phasic and tonic components.

Phasic Feature	Description
Npeak	number of significant SCR wrw
AUC	Area under the curve of phasic signal wrw (μS)
peak	maximum amplitude of significant SCRs wrw ¹ (μS)
Tonic Feature	Description
MeanTonic	Mean value of the tonic component wrw (μS)
DiffTonic	MeanTonic difference between post/pre rest sessions (μS)

wrw= within response window (i.e., 5 sec after stimulus)

The differences between the two levels of velocity (i.e., $V1 = 9.4$ mm/s, $V2 = 37$ mm/s) were studied using a Wilcoxon signed-rank test, due to the non-Gaussianity of the samples. In particular, p-values from Wilcoxon non-parametric tests were associated with the null hypothesis of equal median values between two velocity levels.

IV. RESULTS

Exemplary EDR and HRV series from one representative subject are shown in Fig. 2. Results from SAM scores, HRV and EDR analyses follow below.

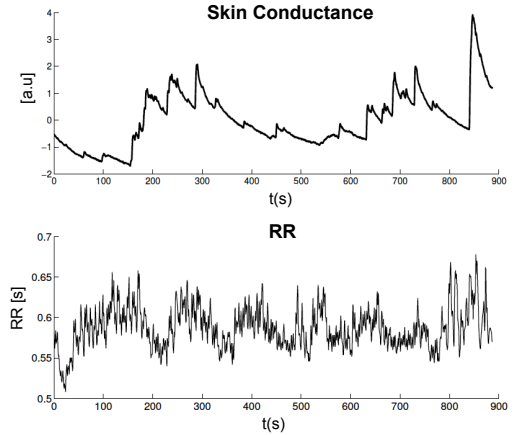


Fig. 2: Exemplary EDR (top panel) and HRV (bottom panel) series from one representative subject.

A. SAM Results

Results from the self-assessment-questionnaire [20] are summarized in Fig. 3 as boxplots. Specifically, statistical analyses revealed that we can associate the stimulus with higher velocity ($V2$) to higher arousal and lower valence (unpleasant) than the caressing stimuli with lower velocity ($V1$), which is coherent with [6].

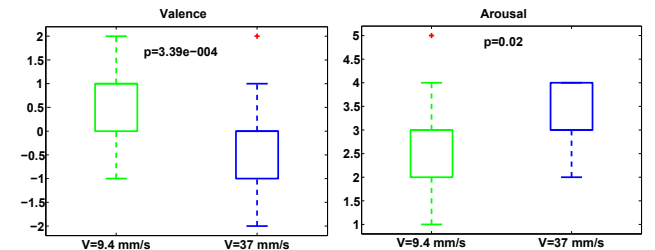


Fig. 3: Comparison of Valence (left) and Arousal (right) values corresponding to two levels of velocities ($V1 = 9.4$ mm/s and $V2 = 37$ mm/s). Red crosses indicate outliers out of the 2nd percentile and the 98th percentile.

B. HRV Results

TABLE II: Mean \pm standard deviation intervals for HRV features. Values were averaged among the subjects. Last column shows p-values from Wilcoxon non-parametric tests, with null hypothesis of equal median values between two velocity levels.

Parameter	V1	V2	p-value
LFHFpw	-1.064 ± 3.857	0.294 ± 2.098	0.031
IVa	-0.677 ± 2.948	1.323 ± 2.535	0.010
IVb	-0.516 ± 2.954	1.613 ± 2.848	0.009
IVa %	1.201 ± 6.144	2.597 ± 5.208	0.015
IVb %	-0.877 ± 6.139	3.323 ± 6.174	0.014
AUC low/tot of SD1	0.001 ± 0.048	-0.024 ± 0.047	0.048
AUC high/tot of SD1	-0.001 ± 0.048	0.0241 ± 0.047	0.048

Features from HRV series were defined considering differential values estimated within sessions of 35 seconds before and after the stimulation. Statistical tests revealed significant differences between the two velocities for seven parameters: one defined in the frequency domain (LF/HF power ratio – LFHFpw, $p < 0.05$), and the others defined through nonlinear methods such as symbolic analysis ($p < 0.03$) and LPP ($p < 0.05$) (see Table II and Fig. 4). We found no significant differences for the other cases.

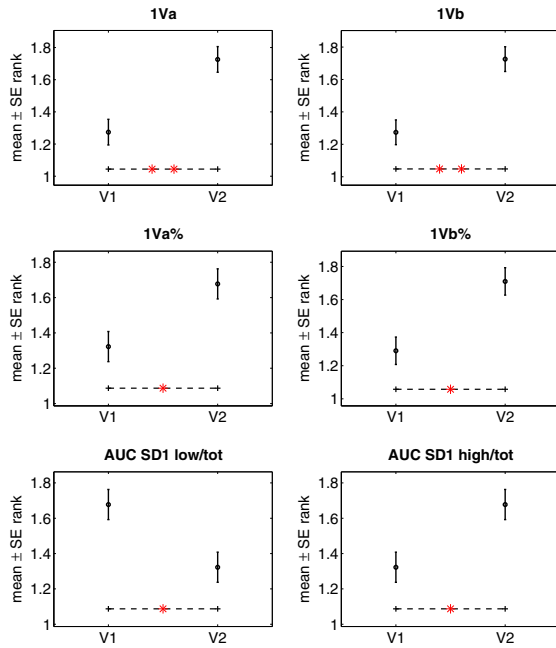


Fig. 4: The dots mark the across-subject mean of the within-subject-rank for each velocity level for each non-linear HRV feature. The whiskers indicate the standard error. The Wilcoxon test revealed significant differences in the cases indicated by asterisks. Legend: (*) $0.01 < y < 0.05$; (**) $0.001 < y \leq 0.01$; (***) $y \leq 0.001$

C. EDR Results

According to the methodology described above, EDR dynamics was studied through its tonic and phasic components. Concerning features of the tonic component, both *MeanTonic* ($p < 0.05$) and *DiffTonic* ($p < 0.001$) showed significant differences between the two caressing velocities. Higher values were associated with caressing performed at higher

velocity (see Table III and Fig. 5(left)). Same trend was also found studying features of the phasic component, where *AUC* and the *Npeak* features revealed a significant difference in relation to the two velocities ($p < 0.001$, see Table III and Fig. 5). No significant differences were found for the other cases.

TABLE III: Mean \pm standard deviation intervals for EDR features. Values were averaged among the subjects. Last column shows p-values from Wilcoxon non-parametric tests, with null hypothesis of equal median values between two velocity levels.

Feature	V1	V2	p-value
Npeak	0.375 ± 0.701	0.969 ± 1.112	0.00048
AUC	0.274 ± 0.397	0.783 ± 1.620	$2.71e-07$
MeanTonic	3.415 ± 5.459	3.495 ± 5.418	0.02
DiffTonic	-0.120 ± 0.256	0.0397 ± 0.265	0.00057

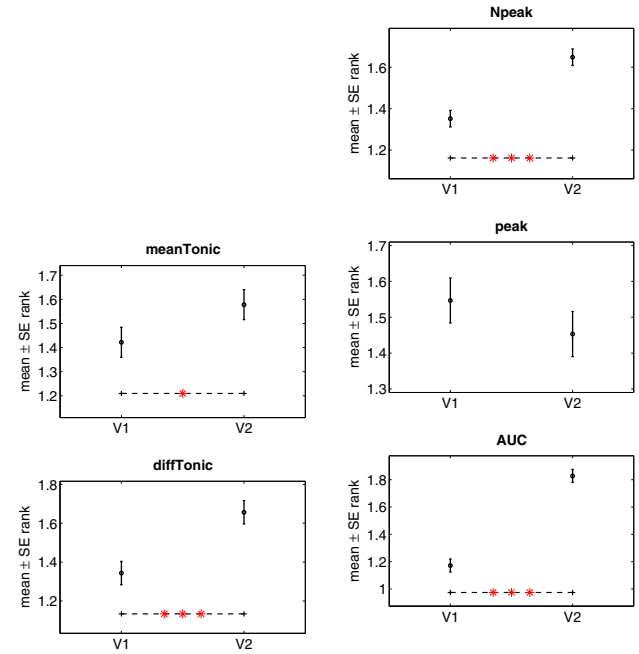


Fig. 5: The dots mark the across-subject mean of the within-subject-rank for each velocity level for each EDR feature, while the whiskers indicate the standard error. The Wilcoxon test revealed significant differences in the cases indicated by asterisks. Legend: (*) $0.01 < y < 0.05$; (**) $0.001 < y \leq 0.01$; (***) $y \leq 0.001$

V. DISCUSSION AND CONCLUSIONS

With this study, we have demonstrated that it is possible to discriminate different caressing stimuli associated to two levels of velocities, through the analysis of physiological signals such as EDR and HRV series. Importantly, the study of SAM scores has revealed that caressing performed at different velocities were associated to two different arousing and pleasantness levels. Particularly, caresses performed at lower velocity were associated to low arousal and high valence (pleasant) levels.

These outcomes confirm and further sustain the results from our preliminary studies devoted to investigate ANS activation through haptic stimulation [11], [36], [37]. Furthermore, it is worth to note that HRV and EDR series are complementary, since they refer to two different dynamics

underlying ANS activity. Indeed, while EDR signal is largely dependent on sympathetic functions, HRV series is representative of parasympathetic ones (through HRV $HF_{power\%}$) [15]. Therefore, our findings suggest that caress-like stimuli can affect both these types of ANS functions, which can be integrated in automatic machine learning systems for the discrimination of physical and affective properties of haptic stimuli. This point will be investigated as future work

At the same time, the here presented results open a fascinating novel perspective for the design of haptic interfaces that integrate affective physiology for HRI. In this envisioned scenario, ANS-related measurements could be used to assess user's comfort and emotional state in interacting with a given haptic device. Furthermore, relying on the *emotional characterization* we performed and we will further develop, we could devise design and control guidelines for a novel generation of haptic systems, which can be commanded to elicit a given emotional state, or in response to a given emotional state of users. The main elements of this paradigm are depicted in Fig. 6. During the administration of haptic stimuli, physiological signals related to ANS dynamics (e.g. the HRV series, respiration dynamics, electrodermal response etc.) can be recorded and analyzed to infer information on user's emotional status and other parameters, e.g. stress, fatigue, etc. (see e.g. [38]).

An interesting point is that these results are consistent across subjects, and hence they can be generalized and effectively employed for a large class of human-machine systems. Of note, although these results were obtained with haptic devices, conclusions from this study can be concretely applied to other robotic devices for HRI, for example in the field of rehabilitation robotics and prosthetics. In these cases, the main goal is to estimate subtler but important aspects such as stress, fatigue, and motivation in patients during training and regular use of robotic aids, thus contributing to correctly assess rehabilitative or assistive procedures, with a high potential impact on acceptability and effectiveness. A particular application case of these results could be the field of shared-control for assistive architectures, where some degree of robotic autonomy or automated help is available to assist the user [39], [40]. What is challenging in this type of HRI is to properly and easily switch from robot to user's control, based on user's needs. In this envisioned novel scenario, where the physiological counterpart will be suitably integrated within the system architecture, it could be easier to detect user's comfort in HRI, thus enabling to switch control in a more naturalistic manner.

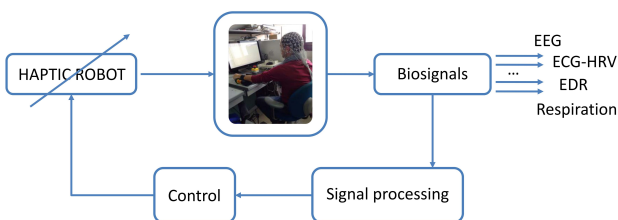


Fig. 6: The main components of the novel paradigm for haptic interfaces, integrating affective physiology within the control loop

ACKNOWLEDGMENTS

This work is supported in part by the European Research Council under the Advanced Grant SoftHands “A Theory of Soft Synergies for a New Generation of Artificial Hands” (no. ERC-291166), by the EU FP7 project “WEARable HAPTics for Humans and Robots (WEARHAP)” (no. 601165) and by the EU H2020 project “SoftPro: Synergy-based Open-source Foundations and Technologies for Prosthetics and RehabilitatiOn” (H2020-ICT-688857).

REFERENCES

- [1] M. J. Hertenstein, “Touch: Its communicative functions in infancy,” *Human Development*, vol. 45, no. 2, pp. 70–94, 2002.
- [2] V. B. Mountcastle, *The sensory hand: neural mechanisms of somatic sensation*. Harvard University Press, 2005.
- [3] F. McGlone, J. Wessberg, and H. Olausson, “Discriminative and affective touch: sensing and feeling,” *Neuron*, vol. 82, no. 4, pp. 737–755, 2014.
- [4] M. T. Fairhurst, L. Löken, and T. Grossmann, “Physiological and behavioral responses reveal 9-month-old infants sensitivity to pleasant touch,” *Psychological science*, vol. 25, no. 5, pp. 1124–1131, 2014.
- [5] A. Klöcker, C. M. Oddo, D. Camboni, M. Penta, and J.-L. Thonnard, “Physical factors influencing pleasant touch during passive fingertip stimulation,” 2014.
- [6] G. K. Essick, F. McGlone *et al.*, “Quantitative assessment of pleasant touch,” *Neuroscience & Biobehavioral Reviews*, vol. 34, no. 2, pp. 192–203, 2010.
- [7] A. C. May, J. L. Stewart, S. F. Tapert, and M. P. Paulus, “The effect of age on neural processing of pleasant soft touch stimuli,” *Frontiers in behavioral neuroscience*, vol. 8, 2014.
- [8] D. Tsetserukou, “Haptihug: A novel haptic display for communication of hug over a distance,” in *Haptics: Generating and Perceiving Tangible Sensations*. Springer, 2010, pp. 340–347.
- [9] S. Yohanan and K. E. MacLean, “The role of affective touch in human-robot interaction: Human intent and expectations in touching the haptic creature,” *International Journal of Social Robotics*, vol. 4, no. 2, pp. 163–180, 2012.
- [10] E. Gatti, G. Caruso, M. Bordegoni, and C. Spence, “Can the feel of the haptic interaction modify a user’s emotional state?” in *World Haptics Conference (WHC), 2013*. IEEE, 2013, pp. 247–252.
- [11] M. Bianchi, G. Valenza, A. Serio, A. Lanata, A. Greco, M. Nardelli, E. P. Scilingo, and A. Bicchi, “Design and preliminary affective characterization of a novel fabric-based tactile display,” in *Haptics Symposium*. IEEE, 2014, pp. 591–596.
- [12] J. Posner, J. A. Russell, and B. S. Peterson, “The circumplex model of affect: An integrative approach to affective neuroscience, cognitive development, and psychopathology,” *Development and psychopathology*, vol. 17, no. 03, pp. 715–734, 2005.
- [13] G. Valenza, A. Lanata, and E. P. Scilingo, “Oscillations of heart rate and respiration synchronize during affective visual stimulation,” *Information Technology in Biomedicine, IEEE Transactions on*, vol. 16, no. 4, pp. 683–690, 2012.
- [14] R. Calvo, S. D’Mello *et al.*, “Affect detection: An interdisciplinary review of models, methods, and their applications,” *Affective Computing, IEEE Transactions on*, vol. 1, no. 1, pp. 18–37, 2010.
- [15] U. R. Acharya, K. P. Joseph, N. Kannathal, C. M. Lim, and J. S. Suri, “Heart rate variability: a review,” *Medical and biological engineering and computing*, vol. 44, no. 12, pp. 1031–1051, 2006.
- [16] L. Lindgren, S. Lehtipalo, O. Winsö, M. Karlsson, U. Wiklund, and C. Brulin, “Touch massage: a pilot study of a complex intervention,” *Nursing in critical care*, vol. 18, no. 6, pp. 269–277, 2013.
- [17] W. Boucsein, *Electrodermal activity*. Springer Science & Business Media, 2012.
- [18] L. S. Löken, M. Evert, and J. Wessberg, “Pleasantness of touch in human glabrous and hairy skin: order effects on affective ratings,” *Brain research*, vol. 1417, pp. 9–15, 2011.
- [19] G. Valenza, L. Citi, A. Lanata, E. P. Scilingo, and R. Barbieri, “Revealing real-time emotional responses: a personalized assessment based on heartbeat dynamics,” *Scientific reports*, vol. 4, 2014.
- [20] M. M. Bradley and P. J. Lang, “Measuring emotion: the self-assessment manikin and the semantic differential,” *Journal of behavior therapy and experimental psychiatry*, vol. 25, no. 1, pp. 49–59, 1994.
- [21] G. Valenza, A. Lanata, and E. P. Scilingo, “The role of nonlinear dynamics in affective valence and arousal recognition,” *Affective Computing, IEEE Transactions On*, vol. 3, no. 2, pp. 237–249, 2012.

- [22] A. Goshvarpour, A. Goshvarpour, and S. Rahati, "Analysis of lagged poincare plots in heart rate signals during meditation," *Digital Signal Processing*, vol. 21, no. 2, pp. 208–214, 2011.
- [23] E. Tobaldini, A. Porta, S.-G. Wei, Z.-H. Zhang, J. Francis, K. R. Casali, R. M. Weiss, R. B. Felder, and N. Montano, "Symbolic analysis detects alterations of cardiac autonomic modulation in congestive heart failure rats," *Autonomic Neuroscience*, vol. 150, no. 1, pp. 21–26, 2009.
- [24] S. Guzzetti, E. Borroni *et al.*, "Symbolic dynamics of heart rate variability a probe to investigate cardiac autonomic modulation," *Circulation*, vol. 112, no. 4, pp. 465–470, 2005.
- [25] M. Brennan, M. Palaniswami, and P. Kamen, "Do existing measures of poincare plot geometry reflect nonlinear features of heart rate variability?" *Biomedical Engineering, IEEE Transactions on*, vol. 48, no. 11, pp. 1342–1347, 2001.
- [26] P. Contreras, R. Canetti, and E. R. Migliaro, "Correlations between frequency-domain hrv indices and lagged poincaré plot width in healthy and diabetic subjects," *Physiological measurement*, vol. 28, no. 1, p. 85, 2007.
- [27] A. Greco, A. Lanata *et al.*, "On the deconvolution analysis of electrodermal activity in bipolar patients." *Proceedings of the 34th IEEE EMBS Conference*, vol. 2012, pp. 6691–6694, 2012.
- [28] A. Greco, A. Lanata, G. Valenza, E. P. Scilingo, and L. Citi, "Electrodermal activity processing: A convex optimization approach," in *Engineering in Medicine and Biology Society (EMBC), 2014 36th Annual International Conference of the IEEE*. IEEE, 2014, pp. 2290–2293.
- [29] M. E. Dawson, A. M. Schell, and D. L. Fillion, "7 the electrodermal system," *Handbook of psychophysiology*, vol. 159, 2007.
- [30] D. R. Bach and M. Staib, "A matching pursuit algorithm for inferring tonic sympathetic arousal from spontaneous skin conductance fluctuations," *Psychophysiology*, vol. 52, no. 8, pp. 1106–1112, 2015.
- [31] M. Benedek and C. Kaernbach, "Decomposition of skin conductance data by means of nonnegative deconvolution," *Psychophysiology*, vol. 47, no. 4, pp. 647–658, 2010.
- [32] A. Greco, G. Valenza, A. Lanata, E. Scilingo, and L. Citi, "cvxeda: a convex optimization approach to electrodermal activity processing," *Biomedical Engineering, IEEE Transactions on*, 2015.
- [33] A. Greco, G. Valenza, M. Nardelli, M. Bianchi, A. Lanata, and E. P. Scilingo, "Electrodermal activity analysis during affective haptic elicitation," in *Engineering in Medicine and Biology Society (EMBC), 2015 37th Annual International Conference of the IEEE*. IEEE, 2015, pp. 5777–5780.
- [34] W. T. Roth, M. E. Dawson, and D. L. Fillion, "Publication recommendations for electrodermal measurements," *Psychophysiology*, vol. 49, pp. 1017–1034, 2012.
- [35] M. Benedek and C. Kaernbach, "A continuous measure of phasic electrodermal activity," *Journal of neuroscience methods*, vol. 190, no. 1, pp. 80–91, 2010.
- [36] A. Greco, G. Valenza *et al.*, "Electrodermal activity analysis during affective haptics elicitation," in *Proceedings of 2015 EMBS Conference*. IEEE, In Press.
- [37] M. Nardelli, G. Valenza *et al.*, "Gender-specific velocity recognition of caress-like stimuli through nonlinear analysis of heart rate variability," in *Proceedings of 2015 EMBS Conference*. IEEE, In Press.
- [38] W. Langewitz and H. Rüdgel, "Spectral analysis of heart rate variability under mental stress." *Journal of hypertension. Supplement: official journal of the International Society of Hypertension*, vol. 7, no. 6, pp. S32–3, 1989.
- [39] G. Niemeyer, C. Preusche, and G. Hirzinger, "Telerobotics," in *Springer handbook of robotics*. Springer, 2008, pp. 741–757.
- [40] S. Javdani, J. A. Bagnell, and S. Srinivasa, "Shared autonomy via hindsight optimization," *arXiv preprint arXiv:1503.07619*, 2015.